Biosensors and Bioelectronics 53 (2014) 288–294

Contents lists available at ScienceDirect

Biosensors and Bioelectronics

journal homepage: www.elsevier.com/locate/bios

A sensitive quartz crystal microbalance assay of adenosine triphosphate via DNAzyme-activated and aptamer-based target-triggering circular amplification

Weiling Song, Zheng Zhu, Yaning Mao, Shusheng Zhang*

Key Laboratory of Biochemical Analysis, Ministry of Education, College of Chemistry and Molecular Engineering, Qingdao University of Science and Technology, Qingdao 266042, PR China

ARTICLE INFO

Article history:
Received 21 June 2013
Received in revised form
17 September 2013
Accepted 26 September 2013
Available online 8 October 2013

Keywords:
Quartz crystal microbalance
Circular amplification
ATP
Aptamers
Gold nanoparticles

ABSTRACT

In this work, a simple and novel quartz crystal microbalance (QCM) assay is demonstrated to selectively and sensitively detect the adenosine triphosphate (ATP). The amplification process consists of circular nucleic acid strand-displacement polymerization, aptamer recognition strategy and nanoparticle signal amplification. With the involvement of an aptamer-based complex, two amplification reaction templates and AuNP-functionalized probes, the whole circle amplification process is triggered by the target recognition of ATP. As an efficient mass amplifier, AuNP-functionalized probes are introduced to enhance the QCM signals. As a result of DNA multiple amplification, a large number of AuNP-functionalized probes are released and hybridized with the capture probes on the gold electrode. Therefore the QCM signals are significantly enhanced, reaching a detection limit of ATP as low as 1.3 nM. This strategy can be conveniently used for any aptamer-target binding events with other biological detection such as protein and small molecules. Moreover, the practical determination of ATP in cancer cells demonstrates the feasibility of this QCM approach and potential application in clinical diagnostics.

1. Introduction

Recently, DNA aptamers and DNAzymes have received considerable attention in chemical–biological research (Yim et al., 2005; Xiao et al., 2012; Pavlov et al., 2005; Fu et al., 2011). Both of them are synthetic DNA molecules with the advantages of easy synthesis, versatility in modification and straightforward sequence-specific recognition. DNA aptamers have been produced for the recognition of targets ranging from small molecules to large proteins and even cells (Liu et al., 2012; Thomas et al., 2012; Hermann and Patel, 2000). Deoxyribozymes (DNAzymes) were discovered through in vitro selection in the 1990s (Robertson and Joyce, 1990), which possess specific catalytic activities and serve as new catalytic tools to achieve signal amplification in ATP detection (Fu et al., 2011). Many DNAzyme-based detection methods with high sensitivity have also been developed to detect small molecular proteins by using enzyme-based amplification strategies, such as nicking enzyme-assisted DNA replication (Weizmann et al., 2006), rolling circle amplification (RCA; Ali and Li, 2009; Cho et al., 2005), and polymerase chain reaction (PCR; Cheglakov et al., 2006).

As the energy substrate for various cellular metabolic functions and the regulator of biological activities, ATP is widely distributed in almost every type of biological cell (Perez-ruiz et al., 2003; Hayashida et al., 2005). It has been also used as an indicator for cell viability and cell injury (Yin et al., 2007; Wang et al., 1996). Therefore, the determination of ATP is essential in biochemical study as well as clinic diagnosis. Several kinds of techniques have been developed for ATP detection in biological samples, including electrochemical detection (Singhal and Kuhr, 1997; Bianchi et al., 1993), imaging techniques (Zhang et al., 2008a, 2008b), fluorescence detection (Kim et al., 2010) and luminescence assay (Wang et al., 2005; Zhou et al., 2006). Electrochemical detection including square-wave voltammetry and cyclic voltammetry has been used to quantify purine base nucleic acids, including ATP, with improved sensitivity (Wang et al., 2000). Other detection methods such as imaging techniques, fluorescence detection or luminescence assay require the labeled signal probes with lower limit of detection, while many biogenic species interfere with the measurement and may lead to ambiguous results.

Quartz crystal microbalance (QCM) as a convenient technique has been widely applied in biochemical analysis with label-free, real-time measurements of interfacial binding reactions (Patel et al., 2009; Papadakis et al., 2010; Wang et al., 2013; Chen et al., 2011; Matsuno et al., 2004). The quartz crystal microbalance system is based on the principle that the resonant frequency shifts

* Corresponding author. Tel./fax: +86 532 8402 2750.
E-mail address: shushzhang@126.com (S. Zhang).

0956-5663/$ - see front matter © 2013 Elsevier B.V. All rights reserved.
http://dx.doi.org/10.1016/j.bios.2013.09.067

of a piezoelectric crystal are directly proportional to the adsorbed mass (Rickert et al., 1997; Bizet et al., 2000). The QCM sensors are highly precise, stable and sensitive for subnanomolar quantities (O'Sullivan and Guilbault, 1999). It provides kinetic information about the adsorption process as well as on the surface coverage of the resulting adsorbed layer. Kinetic parameters can be obtained from the shape of the frequency/time profiles whereas the amount of adsorbed compound is calculated from the total decrease in frequency. There are two main detection methods of delivering the analyte onto the QCM electrode and measuring changes in the resonant frequency of the quartz (Cheng et al., 2012). One method is named the "dip and dry" which calculates the change in resonant frequency of the crystal by measuring the resonance frequency of the crystal twice: once before and once after the target analyte has bound to the probe immobilized on the QCM device. The second method to deliver an analyte and measure frequency changes involves flow injection analysis (FIA) systems. Small volumes of sample are introduced onto the electrode by the FIA system. Changes in the resonant frequency of the crystal are then measured by an oscillator circuit that is linked to a frequency counter, which is connected to the computer. This method is able to perform online analyses of data and gather real-time data, which facilitates the study of binding systems of low-to-high affinities. As a highly sensitive mass detector, QCM is applied in single nucleotide polymorphisms (SNPs) detection (Wang et al., 2012), mismatch recognition (Su et al., 2004), antibody/antigen reaction (Uludag and Tothill, 2012), cell–surface interactions (Pan et al., 2010), and other nanomaterials with 3D structures and multilayers (Orski et al., 2013; Carrigan et al., 2005). Throughout the binding reaction, frequency and energy dissipation are measured by QCM. The QCM biosensor shows low sensitivity to direct detection of single strand DNA by hybridization without further signal amplification.

In the present study, a novel DNAzyme circular amplification and aptamer recognition strategy combined with QCM assay was applied to detect ATP for the first time. The nanoparticles were employed as an efficient mass amplifier and captured with the modified gold electrode. The amplification device involved circular nucleic acid strand-displacement polymerization, aptamer recognition strategy and DNAzyme signaling amplification. In the presence of ATP, it bound to the aptamer in a complex and the template was exposed. Then, the primers were added to hybridize with the exposed sequence, the DNA duplex was formed and the ATP molecule was displaced by the polymerase with strand-displacement activity. The formation of the double-stranded recognition region of nicking endonuclease led to scission of the other primer. Then the scissored primers were added to MB–AuNPs biocomplex and hybridized, with the help of polymerase and nicking endonuclease, and a large number of AuNP-functionalized probes were released. The released AuNP-functionalized probes were hybridized with the capture probes, which enhanced the frequency shift. In this assay, when ATP was added, a two-cycle amplification process was triggered by the aptamer recognition of a target molecule. Due to the high amplification efficiency, a detection limit of 1.3 nM was achieved. In addition, the ATP level in cancer cells (Ramos cells) could be obtained by this method.

2. Experimental

2.1. Materials and reagents

IAll synthesized and HPLC-purified sequences of oligonucleotides as depicted in Table S1 were ordered from Sangon Biotech Co., Ltd. (Shanghai, China). Klenow fragment of *E. coli* DNA polymerase I (5 IU μL^{-1}, denoted as "polymerase" for short), endonuclease (Nb. Bbv CI) and a mixture of four dNTPs (2.5 mM for each component) were purchased from TaKaRa Bio Inc. 1-ethyl-3-(3-dimethylaminopropyl)carbodiimide (EDC), hydrogen tetrachloroaurate (III) tetrhydrate ($HAuCl_4 \cdot 4H_2O$) and trisodium citrate were ordered from Sigma-Aldrich. Streptavidin (SA) was purchased from Sangon Biotech Co., Ltd. (Shanghai, China). Hydrogen peroxide (30%) and ammonia–water (25%) were of analytical reagent grade from Chemical Works of Laiyang Economic Development Zone (Shandong, China). All DNA samples and SA were prepared by dissolving in PBS buffer (0.01 M, pH 7.4). Deionized water was used in all experiments. Microbeads coated with carboxyl groups (COOH–MBs) were purchased from Tianjin BaseLine Chro Tech Research Centre (China). ATP, CTP, GTP, and UTP were purchased from Sigma-Aldrich and stock solutions (1.0 mM) were prepared by using deionized water.

2.2. Apparatus and methods

Transmission electron microscopy (TEM) images were taken with a JEOL JSM-1200EX instrument (Hitachi). Ultraviolet–visible (UV–vis) spectra were measured on a Cary 50 Ultraviolet spectrophotometer (Varian Pty Ltd., Australia). Non-denaturing polyacrylamide gel electrophoresis (PAGE) was carried out on a Tanon VE-180 cell with the Tanon EPS-300 power supply (Tanon Science & Technology Co., Ltd., Shanghai, China), and the PAGE patterns were imaged on a WD-9413B gel imaging system (Beijing Liuyi Instrument Factory, Beijing, China). Atomic Force Microscopy (AFM) image was taken with a Being Nano-Instruments CSPM-4000 (Benyuan, China). A Q-Sense E1 QCM-D instrument (Q-Sense AB, Västra Frölunda, Sweden) was used for the assay, which can provide real-time responses of multiovertone frequencies. The gold-coated quartz crystal with a fundamental resonant frequency of 5 MHz was bought from Q-Sense. Prior to use, the gold electrode surface (Wang et al., 2012) was thoroughly cleaned with piranha solution, a 3:1 mixture of concentrated sulfuric acid and hydrogen peroxide, and then rinsed with deionized water and immersed in a boiling mixture of hydrogen peroxide (30%), ammonia–water (25%), and deionized water with a volume ratio of 1:1:5 for 15 min. The chips were blown with a stream of dry nitrogen gas. A droplet of 30 μL streptavidin was incubated with a gold electrode for approximately 16 h at 4 °C; the gold electrode was washed with deionized water, then immersed into the bio-DNA solution (30 μL, 1×10^{-7} M) for 30 min, washed with deionized water again, and blown dry with nitrogen gas. The frequency shift and the change of the dissipation factor of the crystal were measured in air and in deionized water to check against the standards. After that, the buffer solution was added to the cell and then the released AuNP-functionalized probes solution was flown through the cell under different conditions. When the equilibrium of the solution was reached, buffer solution was flown again to check whether the film was bound to the gold surface chemically. The temperature of the chamber was controlled at 37 °C throughout the experiment.

2.3. Immobilization of DNA onto MBs

IThe process of the immobilization of DNA onto MBs according to the literature (Miao et al., 2008) was enforced as follows: carboxy-modified magnetic microbeads (50 μg) were washed three times with imidazole buffer (50 μL, 0.1 M, pH 6.8) and then activated in the imidazole buffer containing EDC (0.1 M) by gentle shaking for 30 min. DNA S2 (20 μL, 1×10^{-7} M; or DNA S7 (20 μL, 1×10^{-7} M)) was simultaneously added to the activated MBs and the resulting mixture was incubated for 18 h at 37 °C by gentle shaking. The DNA-modified MBs were rinsed three times with buffer (200 mL), magnetically separated and then resuspended in buffer (200 mL) containing BSA (10%) for 1 h to minimize nonspecific adsorption

effects. Then DNA S1 was added to DNA S2 modified MBs; hybridization between the DNA S1 and the DNA S2 modified MBs proceeded for 1 h at 37 °C under gentle agitation. Excess reagents containing noncomplementary DNA were removed by magnetic separation, and the aptamer modified MBs were obtained. The conjugates were then resuspended in buffer (200 mL) before use.

2.4. Preparation of AuNPs, AuNP-functionalized probes and MB–AuNPs biocomplex

The AuNPs were prepared according to the method (Zhang et al., 2008a, 2008b) which has been reported previously. Briefly, $HAuCl_4$ (0.01%) and trisodium citrate (1.0%) solutions were filtered through a 0.22 μm microporous membrane filter, and then the $HAuCl_4$ solution was heated until boiling. By adding 4.0 mL trisodium citrate and stirring for another 10 min, the color of the solution was turned from gray yellow to deep red, and this could indicate the formation of AuNPs. The solution was cooled to room temperature with continuous stirring and stored at 4 °C. The prepared AuNPs were characterized by TEM and UV–visible absorption spectrum.

The process of AuNP-functionalized probes was performed as follows (Taton et al., 2000; Hurst et al., 2006): the mixture of 1.0×10^{-7} M of S8 and 5.0×10^{-6} M of S9 was added to 0.5 mL of freshly prepared AuNPs, shaken gently overnight. After 16 h, the DNA–AuNP conjugates were aged in the solution (0.1 M NaCl, 10 mM acetate buffer) for another 24 h. Excess reagents were removed by centrifuging at 10,000 rpm for 30 min. The precipitate was washed with PBS and centrifuged three times. The resulted nanoparticles were dispersed in PBS for further use. The control AuNP with non-specific sequence was prepared following the process of the AuNP-functionalized probes but only 1.0×10^{-7} M of S8 was added to the freshly prepared AuNPs.

MB–AuNPs biocomplex (Li et al., 2012; Zhang et al., 2010; Ye et al., 2013) was obtained by hybridizing between the AuNP-functionalized probes and DNA-modified MBs. DNA S7 modified MBs were resuspended in 40 μL of PBS buffer and 10 μL of AuNP-functionalized probes. AuNPs were allowed to hybridize with the complementary sequence bound to the MBs for 1 h at 37 °C while shaking gently. After magnetic separation, the reaction mixture was washed three times using PBS buffer. Following the final wash, the mixture was resuspended in PBS for further use.

2.5. Preparation of ATP extracts from cancer cells.

The process of extracting ATP from cancer cells was performed as follows (Zhang et al., 2009, 2010): the Ramos Burkitt's lymphoma cells were cultured in RPMI 1640 medium supplemented with 10% fetal calf serum and 100 IU mL^{-1} penicillin–streptomycin at 37 °C in a humidified atmosphere (95% air and 5% CO_2). The number of cells was determined using a hemocytometer and collected in the exponential phase of growth prior to each experiment. A suspension of Ramos cells was centrifuged at 4000 rpm in cell media buffer, washed with PBS (0.1 M, pH 7.4) three times, and resuspended in 0.25 mL of doubly distilled water. Finally, the cells were disrupted by sonication for 30 min at 0 °C. To remove the homogenate of cell debris, the lysate was centrifuged at 18,000 rpm for 30 min at 4 °C.

2.6. Analysis of ATP

For the detection procedure, different concentrations of ATP were prepared with standard mixed solutions. ATP solution was added to aptamer modified MBs, and then 2.0 μL of Klenow polymerase, 20 μL primer S3 (1.0×10^{-7}M), 20 μL primer S4 (1.0×10^{-7} M) and 2 μL dNTPs (10 mM) were added to perform the strand displacement reaction with cycle amplification. After incubation at 37 °C for 2 h to make the aptamers change their structures to bind ATP, the aptamers bound ATP was released from the modified MBs. The mixture was heated at 80 °C for 20 min to inactivate the Klenow polymerase and magnetically separated. The supernatant was removed and the resulting precipitate contained double-stranded complementary DNA modified MBs which were formed from the above operation. The resulting precipitate was washed three times and then dispersed in PBS. Then the resulting solution containing double-stranded complementary DNA modified MBs, 2.0 μL of endonuclease, 2.0 μL of Klenow polymerase, 2 μL dNTPs (10 mM), and MB–AuNPs biocomplex was added to perform another strand displacement reaction. The mixture was incubated at 37 °C for 2 h, and then all the enzymes were inactivated. The MBs were separated by magnetic force and the AuNP-functionalized probes were obtained after centrifugation.

2.7. Nondenaturing polyacrylamide gel electrophoresis (PAGE)

IThe samples produced in the process of the two cycles amplification reaction were characterized by a 15% nondenaturing polyacrylamide gel electrophoresis (PAGE) analysis (Acr=acrylamide, Bis=N, N′-methylenebisacrylamide; Acr/Bis =29/1). Tris-acetate-EDTA (TAE) (pH=8.5) was used as the separation buffer and the PAGE was carried out at 120 V for 2 h with loading of 9 μL of each sample into the lanes.

3. Results and discussion

3.1. Configuration and operation of the QCM assay

Nicking endonuclease is capable of recognizing specific nucleotide sequences in double-stranded DNA and cleaving one of the two strands (Zhang et al., 2011; Song et al., 2010). With the cooperation of polymerase and nicking endonuclease, the configuration and operation of the QCM assay are illustrated in Scheme 1. For convenient separation, DNA S2 is coupled to magnetic bead A (MB-A) through a covalent interaction between an amino group of S2 and the carboxy group of MB-A. The DNA S1 contains a domain complementary to S2 and an extra unpaired domain in between. After hybridization, the complementary parts form two arms, and the unpaired domain forms a loop in the middle, which results in a bulge-loop structure, denoted as MB-A–S1–S2 complex. A 27-mer ATP aptamer is incorporated into the loop domain and adjacent six nucleotides on the right arm of strand S1, so it can bind ATP molecules when they are added (Xing et al., 2011). The DNA S2 has two encoding regions: a recognition region of nicking endonuclease Nb.BbvCI (–CCTCAGC–, azure) and the residual region is complementary to DNA S1. Primer 1 (S3) and primer 2 (S4) are designed to trigger consecutive reactions which are completely hybridized to the exposed strand of DNA S2 and DNA S1 separately. In the presence of S3 and S4, the DNA duplex (S2/S3) is formed and the ATP molecule is displaced by the polymerase with strand-displacement activity. So the DNA S3 and S4 will trigger cycle 1, which is target recycling-oriented amplification through hybridization with the exposed sequence of substrate and leading to the polymerization on the DNAzyme substrate. Subsequently, the formation of the double-stranded recognition region of Nb.Bbv CI in S2/S3 hybrids will lead to scission of strand S5. The MB–AuNPs biocomplex is added and hybridized with the fragment of S5, and a large number of AuNP-functionalized probes are displaced by the polymerase with strand-displacement activity. The formation of the double-stranded recognition region of Nb.Bbv CI in S5/S7 hybrids will

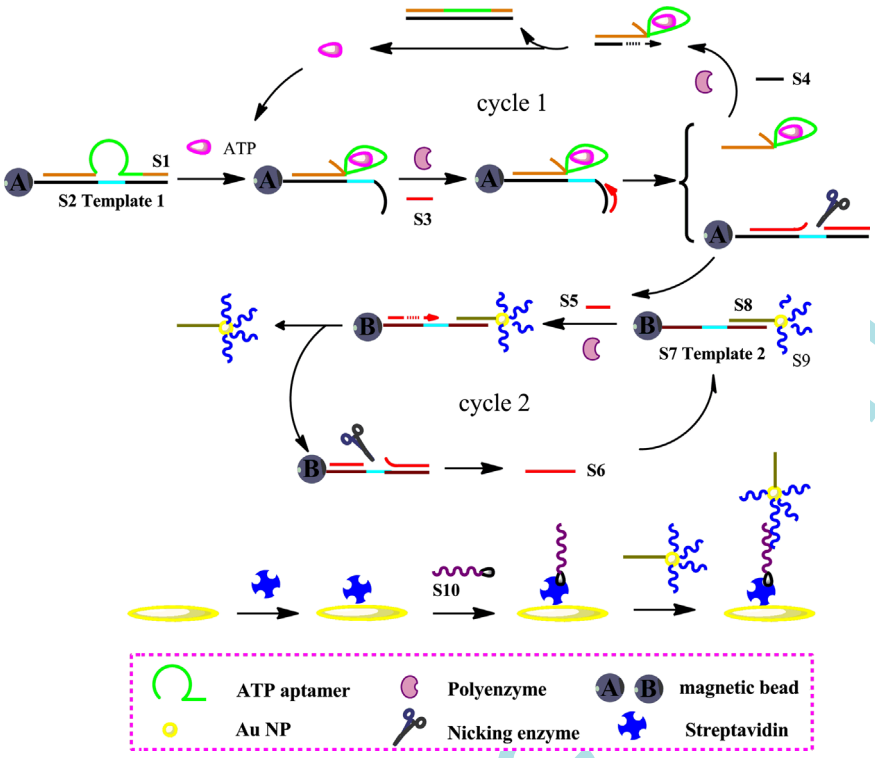

Scheme 1. Schematic representation of ATP detection through DNAzyme-activated two-cycle amplification strategy based on the strand-displacement polymerization activity, which released AuNP-functionalized probes and captured on the QCM biosensor.

lead to scission of strand S6, and then the S6 can hybridize to strand S7 on MB-B to continue the strand-displacement activity. These fragment strands S5 and S6 can trigger cycle 2 under the action of DNAzyme and release a number of AuNP-functionalized probes. DNA capture probes (S10) are biotinylated at the 3′-end in order to achieve oriented immobilization on a streptavidin-covered crystal surface. With two kinds of oligonucleotide immobilized on the surface of nanoparticles, the AuNP-functionalized probes are hybridized with capture probe efficiently which leads to the frequency shift. After accomplishing two cycles amplification, a large number of AuNP-functionalized probes are generated, which stimulate the generation of an enhanced frequency shift. Thus, it is conceivable that the detection sensitivity could be significantly improved.

3.2. Feasibility of the assay

IThe design rationale of this sensing system was verified by the typical result of a real-time frequency shift of amplified QCM biosensor to ATP and control samples, as shown in Fig. 1. The QCM is a piezoelectric mechanosensor whose resonant frequency (ΔF) is sensitive to changes in mass adsorbed on the quartz surface according to the Sauerbrey equation (Sauerbrey, 1959), $\Delta F = -C_f \Delta m$, in which C_f is a constant dependent on the quartz properties, and 56.6 Hz μg^{-1} cm^2 for the 5 MHz AT-cut quartz used here. To demonstrate the feasibility of this approach, a series of control experiments were performed. In the absence of ATP molecule, the right of DNA S2 was not exposed and primers could not hybridize with the template. Therefore the AuNP-functionalized probes were not displaced and the frequency shift was very small (curve a). In the presence of target ATP but no Klenow polymerase or endonuclease, the polymerization reaction could not be performed and the strand S5 was not released, so the cycles would not occur. The results were the same as anticipated and are shown in curve b. Curve c shows the frequency

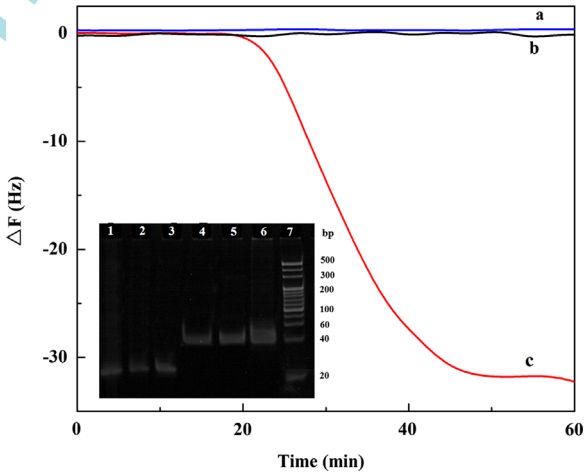

Fig. 1. Real-time frequency shifts of amplified QCM biosensor to control samples: (a) in the absence of target ATP; (b) in the absence of polymerase and the nicking enzyme Nb.Bbv CI; (c) in the presence of target ATP, polymerase, nicking enzyme, and the concentration of ATP is 1.0×10^{-8} M. The concentration of capture probe was 100 nM. Inset: polyacrylamide gel electrophoresis of the system under different conditions: (lane 1: DNA S1/S2 complex; lane 2: DNA S1/S2 complex incubated with ATP for 2 h; lane 3: DNA S1/S2 complex, primers S3 and S4 incubated with ATP for 2 h; lane 4: DNA S1/S2 complex, primers S3 and S4 incubated with ATP for 2 h in the presence of Klenow fragment and dNTPs; lane 5: DNA S1/S2 complex, primers S3 and S4 incubated with ATP for 2 h in the presence of Klenow fragment, dNTPs and Nb.Bbv CI; lane 6: DNA S1/S2 complex, DNA S7/S8 complex, primers S3 and S4 incubated with ATP for 2 h in the presence of Klenow fragment, dNTPs and Nb.Bbv CI; lane 7: DNA marker). The reaction system without the MBs and AuNPs.

shift when ATP, Klenow polymerase and endonuclease coexisted in the reaction system and the larger frequency shift confirmed the feasibility of the assay for detecting ATP.

We also used gel electrophoresis to investigate the viability of our strategy as shown in Fig. 1 (inset). The MBs and AuNPs were

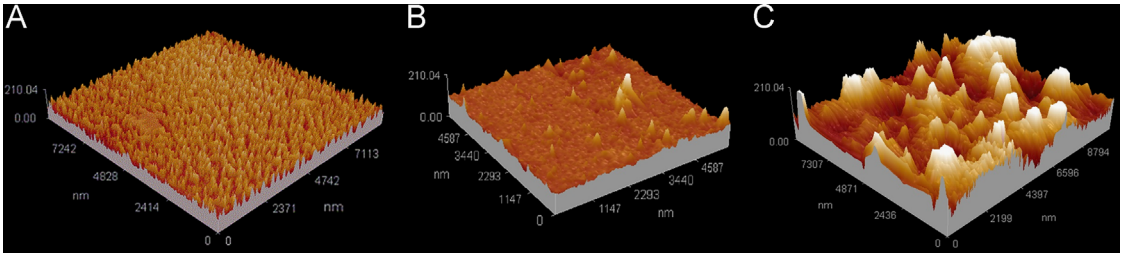

Fig. 2. AFM topography images of the crystal surface. The capture probes immobilized on the surface (A), hybridized with the control AuNP (B) or the released AuNP-functionalized probes (C).

not suitable for PAGE. In lane 1, a migration band between 20 bp and 40 bp which corresponded to the mixture of free DNA S2 and S1 appeared, indicating the formation of the DNA S1/S2 complex. The addition of ATP (lane 2) did not cause an obvious change in band shift compared to the DNA S1/S2 complex which is consistent with the reported paper (Xing et al., 2011). When primers S3 and S4 were added to the mixture, no obvious product was observed (lane 3). However, after the addition of Klenow polymerase and dNTPs to the mixture containing primer S3, primer S4, ATP and DNA S1/S2 complex, the product was shown in lane 4 and a migration band at ~40 bp appeared. This finding suggested that cycle 1 performed well and templates S2 and S1 were converted into dsDNA. Then the nicking endonuclease was added, with no obvious band shift (lane 5) compared to lane 4. In the consequent experiment, the whole amplification reaction was performed using ATP, DNA S1/S2 complex, primer S3, primer S4, Klenow polymerase, dNTPs, nicking endonuclease and DNA S7/S8 complex. The wide bands of lane 6 could be attributed to the multiple components of the whole reaction (e.g., templates S7 and S2 were converted into dsDNA). From the results, the experiments of PAGE could further confirm the feasibility of the proposed assay.

The capability of this surface sensing strategy was further verified by AFM imaging. The capture probes were biotinylated in order to achieve oriented immobilization on the streptavidin-covered crystal surface (Fig. 2A), while the released AuNP-functionalized probes were injected on the surface, shown as numerous "islands" (Fig. 2C), which illustrates that the AuNP-functionalized probes were hybridized with the modified sensor. On the other hand, the smooth surface (Fig. 2B) demonstrates that the control AuNP with non-specific sequence could be hardly hybridized with the modified sensor. The agreement of these data clearly indicated the specificity of the designed capture probes.

3.3. Determination of nonspecific binding to the sensor surface

IThe QCM biosensor is a convenient and valuable tool for real-time monitoring of the interactions (Liu et al., 2006). In order to probe the nonspecific bonding of AuNP-functionalized probes over the capture probes modified surface, the binding experiments were performed with the noncomplementary capture probes, while the released AuNP-functionalized probes were injected on the modified sensor surface. As shown in Fig. S3 (see Supplementary materials), the frequency shift induced by the injection was very limited (about 3 Hz, curve a). In addition, the signal returned by rinsing with the buffer solution. The frequency decreased by about 30 Hz when the released AuNP-functionalized probes were injected into the complementary capture probes modified surface. The frequency did not return to the initial level by rinsing with the buffer solution (curve b) and was significantly higher than in the case of the noncomplementary capture probes. Therefore, it clearly demonstrated that binding occurs through DNA hybridization. Taken all together, these experiments demonstrated that the level of nonspecific bonding of AuNP-functionalized probes onto surfaces modified by a non-complementary DNA sequence was quite low, and easily rectified by rinsing. The QCM was very sensitive to the binding of complementary DNA nanoparticles, and these were not easily removed by rinsing.

3.4. Optimization of the detection conditions

The capture probe is the crucial component for hybrid with AuNP-functionalized probe in this sensing platform (Wang et al., 2012). Hence, the concentration of DNA S10 is a crucial factor for the efficiency of the amplification. On one hand, high concentration of capture probe might increase steric hindrance for the hybridization, leading to a low signal gain. On the other hand, low concentration of capture probe might adversely affect the amplification efficiency because it is not enough to hybridize with AuNP-functionalized probe. Taking this into account, the capture probes of various concentrations (1–1000 nM) were investigated. As shown in Fig. S4, the measured resonant frequency increases with the increase of capture probe concentration from 1.0×10^{-9} M to 1.0×10^{-7} M, and a plateau effect was reached after 1.0×10^{-7} M, which may represent a balance between steric hindrance and hybrid efficiency. Thus, the 1.0×10^{-7} M capture probe was used as an optimal condition.

IThe performance of the ATP detection also depended on the amount of Klenow polymerase and nicking endonuclease, pH value, the temperature, reaction time and proportion of S8 and S9. The amount of Klenow polymerase and nicking endonuclease was optimized, and the results are shown in Figs. S5 and S6. 0.20 U μL^{-1} of Klenow polymerase and 0.1 U μL^{-1} of nicking enzyme were chosen as the optimum amount. The optimal pH value and the temperature were 7.4 and 37 °C, respectively (Figs. S7 and S8). The time of two cycles was investigated; 2 h was chosen as the optimal reaction time for circular cycle 1 and cycle 2 (Fig. S9). The proportion of the signal DNA S8 and DNA S9 was optimized and the ratio of 1:50 was selected for the assays (Fig. S10).

3.5. Sensitivity of the ATP assay

The sensitivity of the detection for ATP was investigated under the optimum condition. ATP standards at different concentrations were analyzed by the proposed method and the results are shown in Fig. 3A. The frequency shifts of AuNP-functionalized probes were in response to samples with different concentrations of ATP. Fig. 3B shows that the frequency shift has a good linear fit to the concentration of the corresponding target ATP in the range from 2.0×10^{-9} M to 1×10^{-8} M. A relative standard deviation (RSD) was calculated to be 4.5% by serially measuring 6.0×10^{-9} M ATP for 11 repetitive determinations, indicating that a high accuracy and reproducibility of the proposed method were acceptable. The detection limit of 1.3 nM was calculated by the triple signal-to-noise method, showing an obvious improvement in sensitivity compared with most existing methods listed in Table S2 (see supplementary materials).

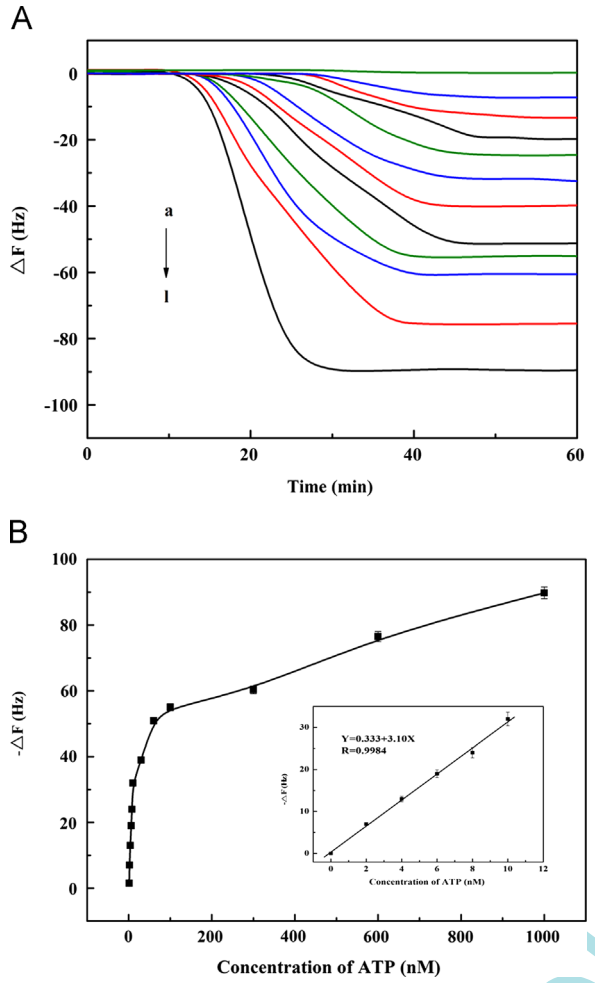

Fig. 3. (A) Real-time frequency responses of amplified QCM biosensor for detection of ATP. The concentrations of ATP (10^{-9} M) were as follows: (a) 0, (b) 2, (c) 4, (d) 6, (e) 8, (f) 10, (g) 30, (h) 60, (i) 100, (j) 300, (k) 600, (l) 1000. (B) Linear relationship between the frequency shifts and the ATP concentrations. Error bars are standard deviation of three repetitive measurements.

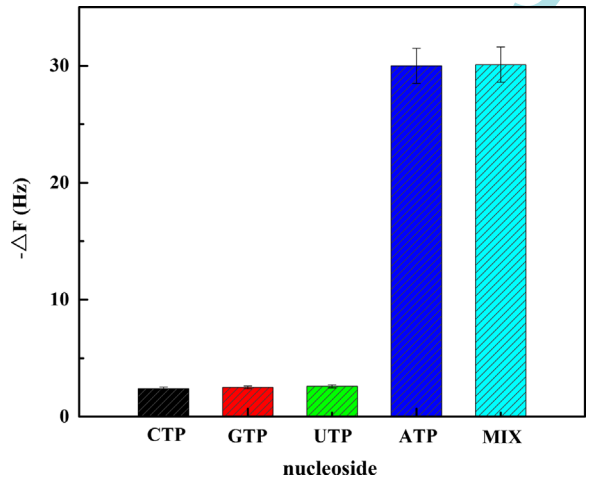

Fig. 4. Frequency responses after the addition of ATP or other nucleosides. The concentration of ATP: 1.0×10^{-8} M. The concentration of CTP, GTP and UTP: 1.0×10^{-6} M.

3.6. Selectivity of the ATP analysis

For the aptamer-based assays, the detection specificity was essentially determined by target recognition ability of the aptamer region. To evaluate this property, control experiments were performed with several ATP analogs: guanidine triphosphate (GTP), cytosine triphosphate (CTP), and uridine triphosphate (UTP). Significantly higher shift of frequency was observed with the target ATP than with its analogs (Fig. 4). When mixed with CTP, GTP and UTP, the frequency shift had no significant change compared with that of ATP, which indicated that these small molecules could not interfere with ATP analysis in the described protocol. These results clearly demonstrated that this method had good selectivity for its target over the same level of its analogs. The non-target molecules did not interfere with the ATP analyses.

Table 1
Analysis of ATP in Ramos cell.

Sample[a]	ATP levels (μM)	RSD (%, $n=3$)	HPLC(μM)	RSD (%, $n=3$)
1	1.03	4.4	1.20	2.9
2	0.93	5.2	0.71	3.3
3	1.10	4.7	1.34	3.6

[a] Each value is the average of three measurements for 10^5 mL^{-1} Ramos cells.

3.7. Practical determination of ATP in Ramos cells

To demonstrate the feasibility of the practical samples analysis of the approach, analysis of cellular ATP from Ramos cells was implemented here. Extracted solutions from Ramos cells were diluted with 100-fold and then analyzed. The results are listed in Table 1 and they show that concentration of ATP in the Ramos cells lysate is 1.02×10^{-6} M (average $\pm$ S.D., $n=3$) per 1×10^5 cells. For comparison, HPLC was conducted for the analysis of the same sample (see Supporting information). The result indicated that the data obtained by HPLC method are consistent with this proposed method. So this method could be used to monitor the content of ATP in cell extracts without the interference of other substance.

3.8. Storage stability of the QCM biosensor

IThe stability of the QCM biosensor was investigated. The QCM biosensor stored by use of 1% sodium azide solution at 4 °C was tested periodically with the 1×10^{-8} M ATP sample. Experiments were performed on seven crystals for measurement continuously for 7 days. The stability was almost fully maintained for the first 4 days and then started to decline. After 6 days, the relative frequency shifts were about 95% compared with its initial response.

4. Conclusion

In summary, the present study has introduced a novel signal amplification strategy for sensitive detection of ATP based on QCM. The detection process consists of a two-cycle mode to amplify signals and make use of the gold nanoparticles as the signal probe, which induce significant enhancement of QCM signals. The method has implemented two kinds of enzymes as a versatile catalyst for the recycling of the analytes. Furthermore, combined with circular nucleic acid strand-displacement polymerization and aptamer recognition strategy, a detection limit of 1.3 nM for ATP was obtained. Due to the high affinity and specificity of aptamer for ATP, this method exhibits successful determination of ATP in cancer cells. Therefore, with its specificity and sensitivity, this system could be expected to be developed into a promising practical assay such as basic research and in vitro diagnostics.

Acknowledgments

This work was supported by the National Natural Science Foundation of China (21025523, 21275086), the National Basic Research Program of China (2010CB732404), and the Program for Changjiang Scholars and Innovative Research Team in University (PCSIRT).

Appendix A. Supplementary material

Supplementary data associated with this article can be found in the online version at http://dx.doi.org/10.1016/j.bios.2013.09.067.

References

Ali, M.M., Li, Y., 2009. Angewandte Chemie International Edition 48, 3512–3515.
Bianchi, A., Domenech, A., Garcia-Espana, E., 1993. Analytical Chemistry 65, 3137–3142.
Bizet, K., Gabrielli, C., Perrot, H., 2000. Applied Biochemistry and Biotechnology 89, 139–149.
Carrigan, S.D., Scott, G., Tabrizian, M., 2005. Langmuir 21, 5966–5973.
Cheglakov, Z., Weizmann, Y., Beissenhirtz, M.K., Willner, I., 2006. Chemical Communications, 3205–3207.
Chen, Q., Wu, X., Wang, D., Tang, W., Li, N., Liu, F., 2011. Analyst 136, 2572–2577.
Cheng, C.I., Chang, Y.P., Chu, Y.H., 2012. Chemical Society Reviews 41, 1947–1971.
Cho, E.J., Yang, L., Levy, M., Ellington, A.D., 2005. Journal of the American Chemical Society 127, 2022–2023.
Fu, R., Li, T., Lee, S.S., Park, H.G., 2011. Analytical Chemistry 83, 494–500.
Hayashida, M., Fukuda, K., Fukunaga, A., 2005. Journal of Anesthesia 19, 225–235.
Hermann, T., Patel, D.J., 2000. Science 287, 820–825.
Hurst, S.J., Lytton-Jean, A.K.R., Mirkin, C.A., 2006. Analytical Chemistry 78, 8313–8318.
Kim, J., Ahn, J., Barone, P., Jin, H., Zhang, J., Heller, D., Strano, M., 2010. Angewandte Chemie International Edition 49, 1456–1459.
Li, Y., Lei, C., Zeng, Y., Ji, X., Zhang, S., 2012. Chemical Communications 48, 10892–10894.
Liu, X., Freeman, R., Willner, I., 2012. Chemistry: A European Journal 18, 2207–2211.
Liu, Y., Tang, X., Pei, J., Zhang, L., Liu, F., Li, K., 2006. Chemistry: A European Journal 12, 7807–7815.
Matsuno, H., Furusawa, H., Okahata, Y., 2004. Chemistry: A European Journal 10, 6172–6178.
Miao, J., Cao, Z., Zhou, Y., Lau, C., Lu, J., 2008. Analytical Chemistry 80, 1606–1613.
Orski, S.V., Kundu, S., Gross, R., Beers, K.L., 2013. Biomacromolecules 14, 377–386.
O'Sullivan, C.K., Guilbault, G.G., 1999. Biosensors and Bioelectronics 14, 663–670.
Pan, Y., Guo, M., Nie, Z., Huang, Y., Pan, C., Zeng, K., Zhang, Y., Yao, S., 2010. Biosensors and Bioelectronics, 1609–1614.
Papadakis, G., Tsortos, A., Gizeli, E., 2010. Nano Letters 10, 5093–5097.
Patel, A.R., Kanazawa, K.K., Frank, C.W., 2009. Analytical Chemistry 81, 6021–6029.
Pavlov, V., Shlyahovsky, B., Willner, I., 2005. Journal of the American Chemical Society 127, 6522–6523.
Perez-ruiz, T., Martine-Lozano, C., Tomas, V., Martin, J., 2003. Analytical and Bioanalytical Chemistry 377, 189–194.
Rickert, J., Brecht, A., Göpel, W., 1997. Biosensors and Bioelectronics 12, 567–575.
Robertson, D.L., Joyce, G.F., 1990. Nature 344, 467–468.
Sauerbrey, G., 1959. Zeitschrift für Physik A: Hadrons and Nuclei 155, 206–222.
Singhal, P., Kuhr, W.G., 1997. Analytical Chemistry 69, 3552–3557.
Song, Q., Wu, H., Feng, F., Zhou, G., Kajiyama, T., Kambara, H., 2010. Analytical Chemistry 82, 2074–2081.
Su, X., Robelek, R., Wu, Y., Wang, G., Knoll, W., 2004. Analytical Chemistry 76, 489–494.
Taton, T.A., Mirkin, C.A., Letsinger, R.L., 2000. Science 289, 1757–1760.
Thomas, J.M., Chakraborty, B., Sen, D., Yu, H.Z., 2012. Journal of the American Chemical Society 134, 13823–13833.
Uludag, Y., Tothill, I.E., 2012. Analytical Chemistry 84, 5898–5904.
Wang, D., Tang, W., Wu, X., Wang, X., Chen, G., Chen, Q., Li, N., Liu, F., 2012. Analytical Chemistry 84, 7008–7014.
Wang, J., Jiang, Y., Zhou, C., Fang, X., 2005. Analytical Chemistry 77, 3542–3546.
Wang, J., Zhu, Z., Ma, H., 2013. Analytical Chemistry 85, 2096–2101.
Wang, Y., Roman, R., Lidofsky, S.D., Fitz, J.G., 1996. Proceedings of the National Academy of Sciences of the United States of America 93, 12020–12025.
Wang, Z., Haydon, P.G., Yeung, E.S., 2000. Analytical Chemistry 72, 2001–2007.
Weizmann, Y., Beissenhirtz, M.K., Cheglakov, Z., Nowarski, R., Kotler, M., Willner, I., 2006. Angewandte Chemie 118, 7544–7548.
Xiao, S.J., Hu, P.P., Xiao, G.F., Wang, Y., Liu, Y., Huang, C.Z., 2012. The Journal of Physical Chemistry B 116, 9565–9569.
Xing, Y., Yang, Z., Liu, D., 2011. Angewandte Chemie International Edition 50, 11934–11936.
Ye, S., Guo, Y., Xiao, J., Zhang, S., 2013. Chemical Communications 49, 3643–3645.
Yin, J., Xu, K.P., Zhang, J., Kumar, A., Yu, F.S.X., 2007. Journal of Cell Science 120, 815–825.
Yim, T.J., Liu, J., Lu, Y., Kane, R.S., Dordick, J.S., 2005. Journal of the American Chemical Society 127, 12200–12201.
Zhang, H., Fang, C., Zhang, S., 2010. Chemistry: A European Journal 16, 12434–12439.
Zhang, H., Fang, C., Zhang, S., 2011. Chemistry: A European Journal 17, 7531–7537.
Zhang, S., Zhong, H., Ding, C., 2008a. Analytical Chemistry 80, 7206–7212.
Zhang, S., Yan, Y., Bi, S., 2009. Analytical Chemistry 81, 8695–8701.
Zhang, Y., Phillips, G.J., Li, Q., Yeung, E.S., 2008b. Analytical Chemistry 80, 9316–9325.
Zhou, G., Kajiyama, T., Gotou, M., Kishimoto, A., Suzuki, S., Kambara, H., 2006. Analytical Chemistry 78, 4482–4489.